MULTIFUNCTIONAL HYBRID COMPOSITE FOR THERMAL PROTECTION OF CARBON FIBER REINFORCED POLYMERS (CFRPS) IN AEROSPACE APPLICATIONS

Tosin D. Ajayi[1], Kyunghoon Kim[1], Jun Liu[1], Bill C. Nickerson[2], Cheryl Xu[1*]

[1] Department of Mechanical and Aerospace Engineering,
North Carolina State University,
911 Oval Drive,
Raleigh, NC 27695

[2] Office of Naval research
875 N Randolph Street,
Arlington, VA 22203

[*] Email: cheryl.xu@ncsu.edu
[*] Tel: 407-227-1372

ABSTRACT

A protective material was developed for carbon fiber reinforced polymer (CFRP) composites to improve their survivability in high temperature environment. This protective material is a carbon nanotube (CNT) reinforced ceramic (CNT/ceramic) thin film and is bonded onto CFRP for the purpose of dissipating heat quickly along in-plane direction instead of burning into the CFRP underneath. The anisotropic thermal conductivity of our CNT/ceramic thin film was investigated using an advanced characterization method called time-domain thermoreflectance (TDTR) method. The measurement results show that the thermal conductivity is 7.2 ± 0.7 W/mK along the in-plane direction, and 2.0 ± 0.2 W/mK along the through-thickness direction. To confirm the simulation results, we designed an experiment based on actual applications by heating the top surface of the sample above 120 °C (maximum service temperature of most CFRP material) and measuring the heat distribution in both the in-plane and through thickness directions. The result proves that our CNT/ceramic thin film can offer protection to CFRP composite for high temperature applications.

1. INTRODUCTION

The aerospace industry's continuous effort to enhance the performance of military and commercial aircraft is a great driving force behind developing improved high performance structural materials [1]. Carbon fiber reinforced polymer (CFRP) composites are one type composite material that is commonly used in aerospace and aviation applications because of their exceptional strength and superior physical properties [2]. However, matrix materials are made of polymers, and that means when they are exposed to hyper-thermal environment, the organic matrix decomposes. For example,

SAMPE Conference Proceedings. Charlotte, NC, May 20-23, 2019. Society for the Advancement of Material and Process Engineering – North America.

epoxy and bismaleimides (BMI) have maximum service temperatures of about 190 ^{o}C and 232 ^{o}C respectively [3]. Therefore, use of these materials at temperature above the maximum service temperature will cause the polymers to start to decompose. The decomposition could lead to delamination of fibers, loss of structural integrity and overall degradation in the mechanical properties of the overall composite material [4,5].

To prevent the aforementioned structural damage, it is necessary to protect the CFRP structure using a thermal barrier coating to elongate the survival time in high temperature applications. For instance, various kinds of thermal barrier coatings have been developed to protect CFRP against adverse thermal environments, with these coatings mostly metal-based [6-8]. However, metals have high isotropic thermal properties and so it becomes more difficult to protect CFRP in high temperature environment such as for aerospace applications. Also, another reason is the large difference in coefficient of thermal expansion (CTE) between the metal and polymer composite which generates residual thermal stresses in the interface during cyclic thermal loading. Ceramic particles have also been used as coatings for CFRP protection due to their excellent thermal insulation properties using spray coating methods [9]. However, coating is not continuous, uneven and also possess rough surface morphology. This degrades the mechanical strength of the CFRP material and undermines its thermal barrier properties.

Therefore, bonding a skin material onto the polymer composites seems like the best way to go about protecting them in adverse conditions. Generally, the most common methods for joining composites together are mechanical joining and adhesively-bonded joining [10]. Mechanical joining uses bolts or rivets to fasten parts which requires drilling of holes. However, drilling operations introduces defects such as delamination as a result of stress concentration around the holes. On the other hand, adhesively-bonding method requires no drilling of holes and also helps distribute the load over a large surface area [11]. Co-curing is a type of adhesively-bonding method that requires curing a composite laminate and simultaneously bonding it to some other uncured material. With this process, the design and fabrication of the structure becomes simpler since the adhesive of the co-cured joint is the same material as the resin of the composite material.

For these reasons, a novel protective skin material made up of carbon nanotube (CNT) reinforced ceramic (CNT/ceramic) thin film was developed, and was bonded (co-curing process) onto CFRP to form a hybrid composite for the purpose of dissipating heat quickly along in-plane direction instead of burning into the CFRP underneath. This protective skin material is expected to slow heat conduction into the CFRP from the thermal environment, thereby improving the CFRP's survivability. Using an advanced characterization method called time-domain thermoreflectance (TDTR), the thermal conductivities of the CNT/ceramic film along the in-plane direction and along the through-thickness direction were measured. To further back up the TDTR characterization, we also experimentally investigated the temperature effect at the interface between the protective system and the CFRP substrate of the hybrid composite when the outermost layer is heated to 125 ^{o}C.

2. EXPERIMENTATION

2.1. Materials and Manufacturing Procedure of the Hybrid Composite

Details of materials and preparation procedures can be found in [12]. Through a careful manufacturing procedure, a hybrid multifunctional composite material is developed where the outermost layer is a CNT composite skin material for enhanced thermal protection. The skin material is a flexible CNT/ceramic film that is bonded onto the outermost layer of CFRP via a co-curing process to form a hybrid composite. This process involves placing multi-layers of non-woven carbon fiber (Cf) tissues acting as the transition layer between CNT/composite film and the CFRP substrate. The transition layer is designed to improve the bonding strength and reduce the coefficient of thermal expansion mismatch between the exterior ceramic composite layer and the CFRP layer. Figure 1 (a) shows the major manufacturing steps to make such a hybrid composite material. The preceramic polymer precursor used in this study is polysilazane (PSZ) which is the precursor of silicon carbon nitride (SiCN) ceramics. After the complete preparation of the hybrid composite, this transition layer is made up of carbon fibers, ceramic and polymer islands held

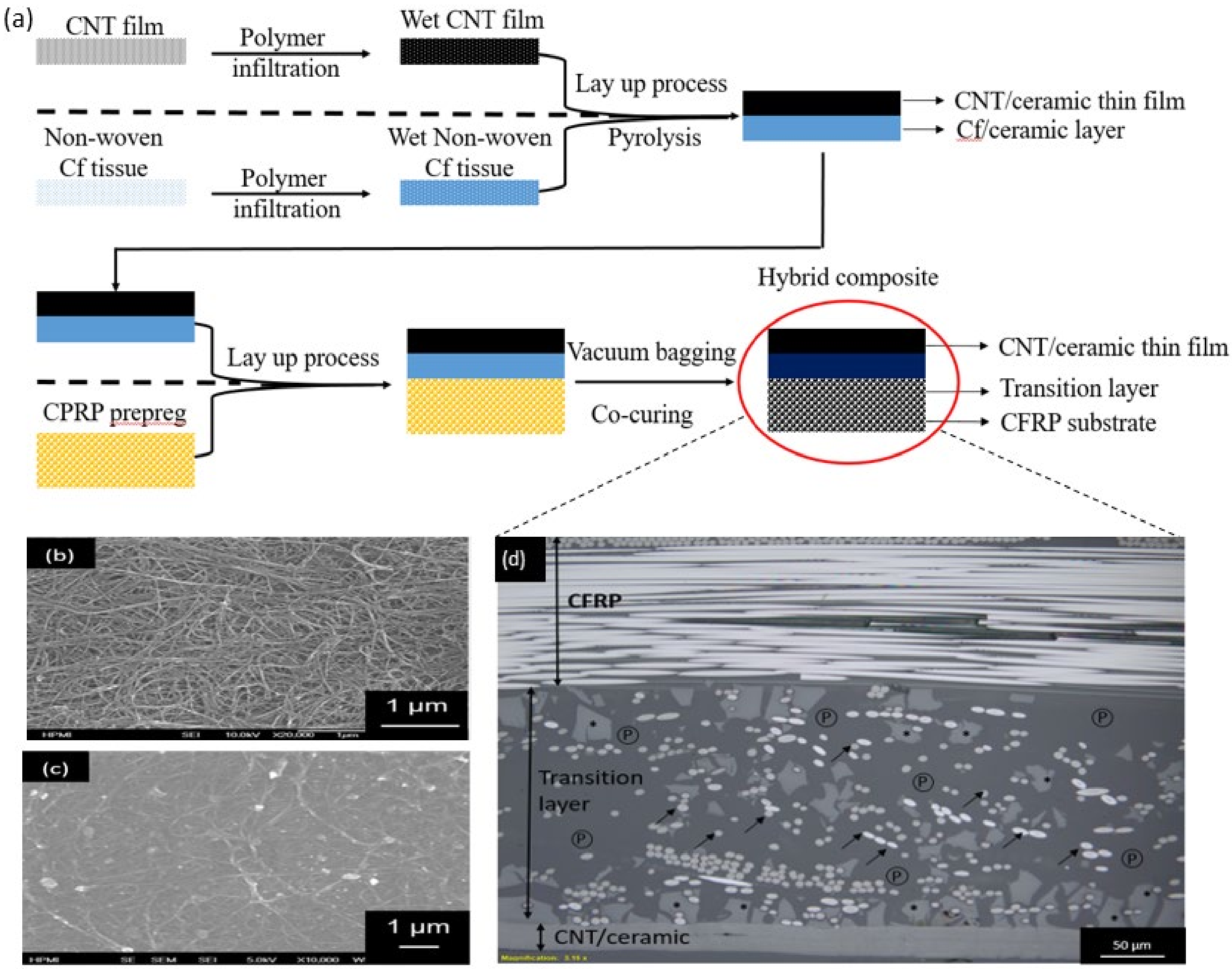

together by interlocking as shown in Figure 1 (d). Figure 1 (b) and 1 (c) show the SEM images of raw CNT preform and the CNT ceramic composite film respectively.

Figure 1: (a) Schematic representation of the preparation procedures for the hybrid composite, SEM micrographs of (b) raw CNT preform and (c) CNT/ceramic composite surface and (d) optical image of the cross-section of hybrid composite showing a small region of the CFRP and complete transition layer and CNT/ceramic layer.

(Arrow sign: cross-section of carbon fiber; *: ceramic matrix; and (P) polymer matrix)

2.2. Thermal Property Measurement

2.2.1. Anisotropic Thermal Property Characterization of CNT/ceramic Thin Film

The anisotropic thermal conductivity of CNT/ceramic thin film was characterized using an advanced characterization method – time-domain thermoreflectance (TDTR) method [13-16]. Conventional approaches to measure thermal conductivity usually require a specific bulk sample with certain shape, and do not consider the anisotropic nature of most materials. In addition, conventional approaches, such as steady-state measurement or laser-flash method, require corrections of heat convection and thermal radiation effect. TDTR method does not need to probe a large volume of the sample, which means that the convection and radiation effects can be negligible. Moreover, the TDTR method can accurately measure anisotropic thermal conductivity

The TDTR method is an ultrafast-laser based non-contact optical method, which is better than methods with detection scheme based on electrical current and voltage signals, such as the 3ω method or hotwire method. The TDTR method uses two laser beams: the pump beam heats a metallic surface coated on the target sample and generates a small temperature rise (<20 K) and the probe beam detects the surface reflectivity change. In a metallic film, the change of optical reflectivity linearly depends on the change of temperature, which is defined by the thermoreflectance coefficient R. With a controllable and variable time delay between the probe beam and the pump beam, the temperature decay in the metallic film can be monitored. The decay rate depends on the thermal properties of the measured materials, which can be obtained by fitting the experimental data with the heat transfer model. The beam size is on the order of 1-10 µm, so this method can probe the local thermal properties on the micron scale. A thermal conductivity map can be obtained by scanning both the pump and probe laser beams on the sample surface. One requirement for the TDTR measurement is a smooth surface with a low surface roughness because this is an optical method. If the surface is rough, the diffuse light will affect the signal. We used ultramicrotome to polish the surface, to which the roughness of the sample can be reduced to 30 nm or even smaller. The team is very experienced in this sample preparation and measurement. Thermal conductivity of different materials have been measured using this method (Figure 2(c)).

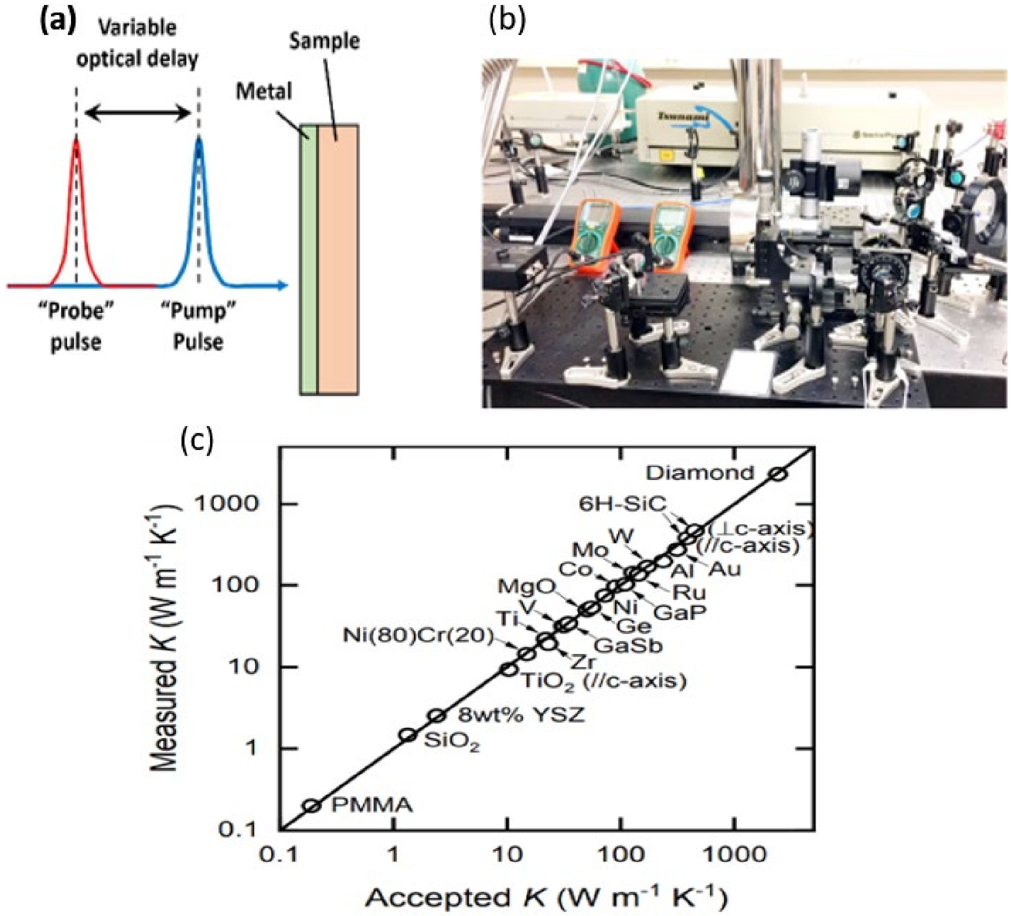

Figure 2: TDTR method for thermal conductivity measurement and mapping. (a) Principles of TDTR method. (b) The TDTR setup at NC State University. (c)The accuracy of TDTR method has been validated by comparing with accepted values [17].

The CNT/ceramic thin film samples were cut using ultramicrotome technique. The samples were placed in superglue and then cut using the ultramicrotome in two directions: one cut exposed the cross-section area (we called this 'parallel' sample) and the other cut exposed the radial surface (we called this 'perpendicular' sample). Figure 3 is the optical image and surface profile of uncut sample, which shows a relatively high surface roughness (~116 nm) and is not suitable for the measurement using TDTR method. Figure 4 is the optical images and surface profile of the cut sample, which clearly shows a smoother sample surface, and the surface roughness is reduced to ~28 nm. Then, ~100 nm Al thin film was deposited using thermal evaporation on top of the sample's surface.

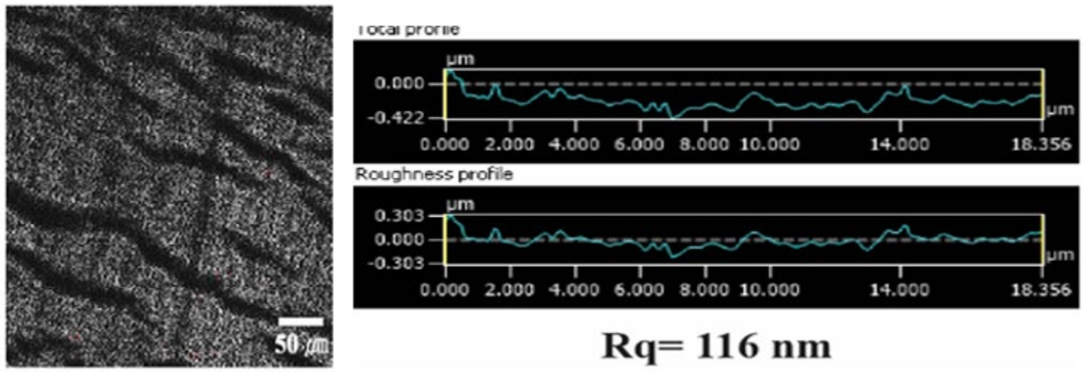

Figure 3: The image and roughness analysis before cutting. The optical image of the CNT/ceramic film samples with 10x objective lens and the surface height-profile image of the samples with 150x objective lens (Rq = 116 nm).

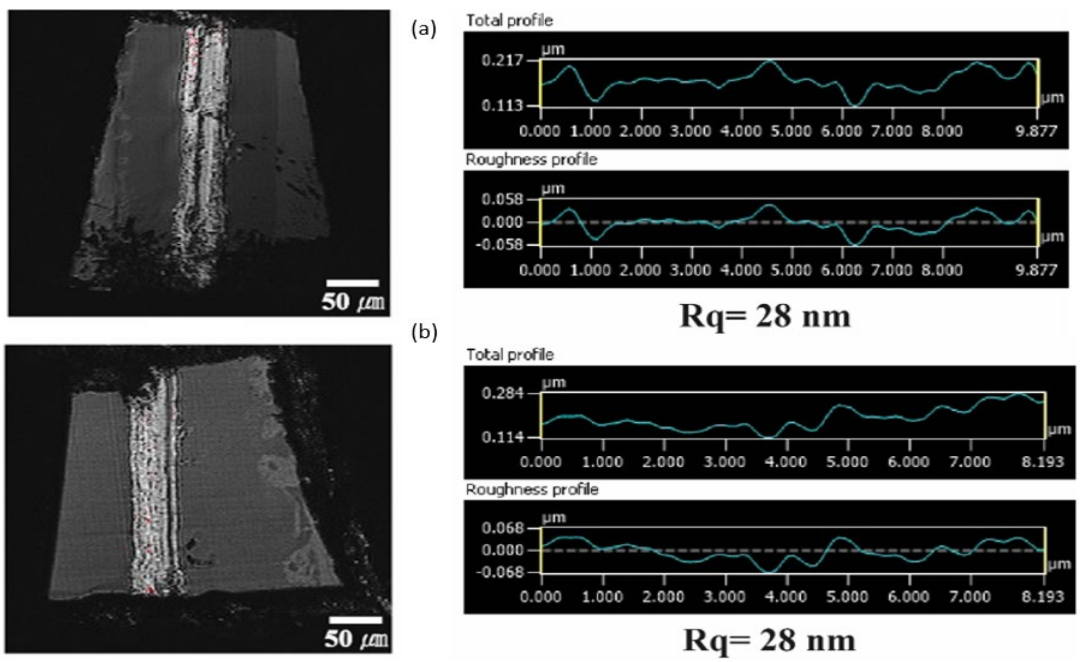

Figure 4: The image and roughness analysis before cutting.
(a) The optical image of the cross-section of cut parallel samples with 10x objective lens;
(b) The optical image of the cross-section of cut perpendicular samples with 10x objective lens.
And the surface height-profile images of the cut parallel and perpendicular samples with 150x objective lens (Rq = 28 nm).

When processing the experimental data, the ratio between the in-phase and out-of-phase signals – V_{in}/V_{out} is usually fitted by the thermal transport model to derive the thermal properties of the sample. The in-phase signal V_{in} represents the surface temperature change as a result of the pulse heating. The decay rate of V_{in} represents the cooling process of sample surface which is due to heat dissipation, and this also directly relates to the thermal diffusivity of the sample. On the other hand, the out-of-phase V_{out}, is due to the modulated continuous heating of the sample [17].

2.2.2. Temperature Measurement at the Interface between Transition Layer and CFRP

Here, we simulated the temperature distribution on the hybrid composite (i.e. when the protective system has been bonded onto CFRP) at the transition layer – CFRP interface when the heat is supplied on the exterior surface of the CNT/ceramic film. To simulate the temperature profile at this interface, we needed to experimentally measure the temperature at a point along the in-plane direction and the temperature at the back of the sample along the through-thickness direction.

For this measurement, we used an experimental approach designed specifically to overcome challenges associated with laboratory thermal measurement such as heat loss through radiation. Here, a circular cartridge heater (Chromalox CIR-1060 ¼" diameter, OMEGA Engineering, INC., Norwalk, CT, US) was attached onto the exterior surface (CNT/ceramic surface) of the sample (1" by 1" in dimension) and then is connected to a heat source (Agilent 6613C DC power supply system). The heat is transferred through the cartridge onto the sample's exterior surface at 135 ^{o}C ± 2 ^{o}C. Thermocouples (OMEGA Engineering) were pinned to the center of the sample's surface with epoxy glue (low conductivity material) and placed at different positions from the heat source (such as 'd' along the in-plane direction) as shown in Figure 5 (a). The thermocouple (TC) placed beside the conductor on the ceramic layer is required to monitor the temperature difference from the heat source and on the surface of the sample and to adjust the heat source parameters if there is a fluctuation. The thermocouples were connected to a thermometer (HH802U OMEGA Engineering) to take the temperature readings and then connected to a data acquisition unit (DAQ) to take the real time temperature readings from each position on the sample. The thermocouple used for this measurement is an unsheathed fine gage micro-temperature thermocouple with 0.1 ^{o}C resolution to ensure its measurement sensitivity.

To properly hold the sample for the measurement, a sample holder and guide built with acrylic plate was used. The guide was assembled in a way that allows the ease of detaching and setting up samples for the measurement. Holes were drilled through the acrylic plates to pass the TCs and the cartridge heater onto the samples surface as shown in the CAD model in Figure 5 (b). The upper guide and the lower guide ensure that the TCs cartridge heater are well guided to have a full contact with the sample. The set up was housed in a styrofoam box to ensure heat loss through radiation was greatly minimized. The placement of the thermocouples determines the direction of thermal property measured (i.e. TC1 and TC2 measured the in-plane temperature and TC3 measured the temperature at the back of the sample in the through-thickness direction).

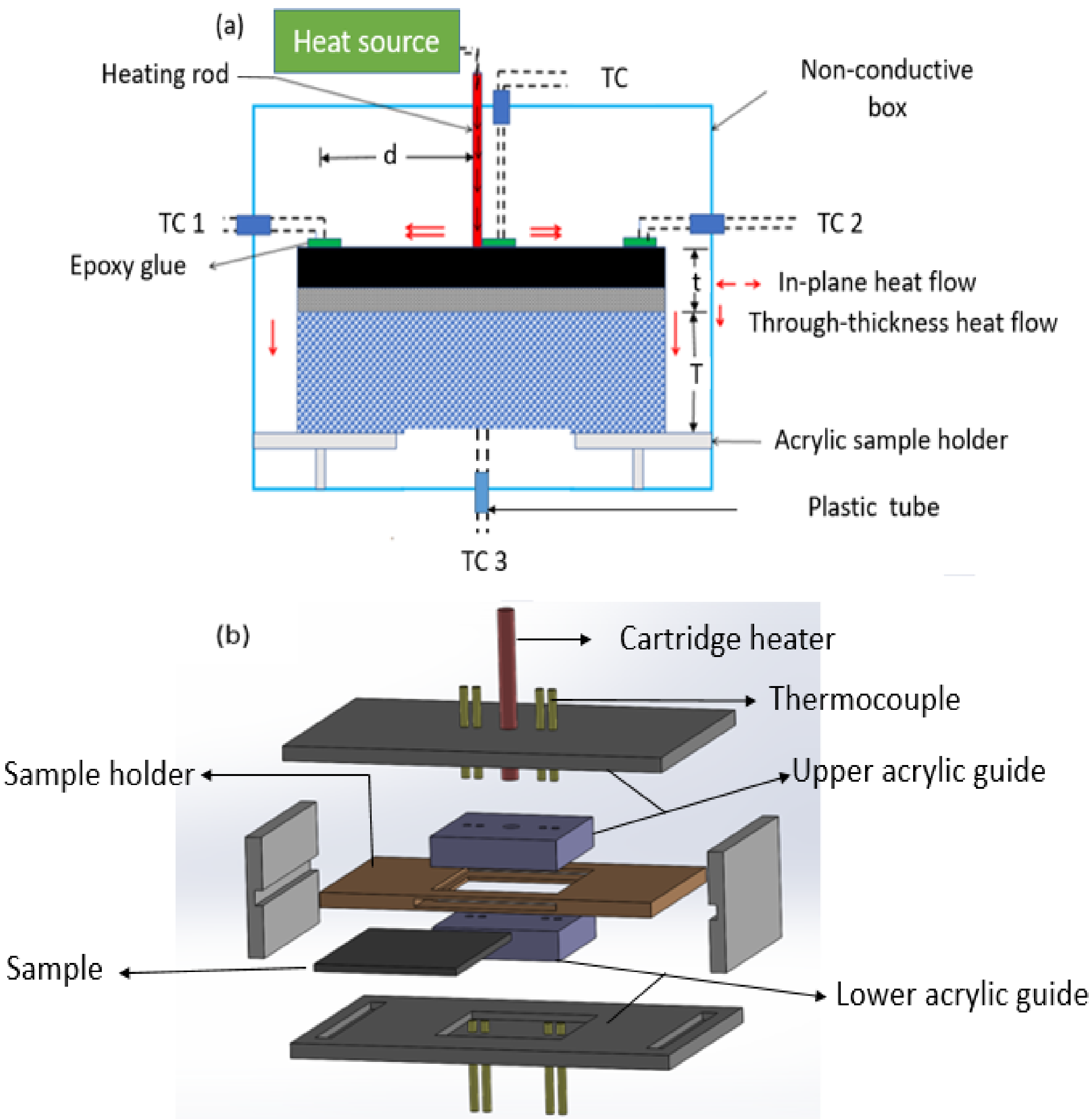

Figure 5: (a) Schematic illustration and (b) CAD model of the set up for the thermal measurement.

3. RESULTS

3.1. Microstructural Investigation

The microstructural properties of the hybrid composite were investigated using both optical microscope (Olympus BX41M-LED) and scanning electron microscopy, SEM (JEOL 7401F). Figure 1 (b) shows the randomly entangled morphology of as-received CNT preform. From the image, the preform is clearly observed to be composed of nanoscale pores (average pore size is around 15 nm), which allows the infiltration of the liquid ceramic precursor (polysilazane). Figure 1 (c) shows the morphology of the structure after conversion to CNT/ceramic composite. The structure shows dense surface even after pyrolysis (densification). Furthermore, the bonding properties of the components in the interface was also characterized. Figure 1 (d) shows optical images of the cross-section of the hybrid composite. The thickness of the CNT/ceramic film and transition layer are about 40 µm and 250 µm respectively. As shown in Figure 1 (d), the transition layer can be clearly seen to be without voids. The layer displays excellent bonding feature especially between ceramic and the polymer part with homogeneous distribution. The carbon fibers in the transition layer (diameter around 10 µm) also bond seamlessly with both the ceramic and the polymer. The observation in the transition layer shows that the interconnectivity of ceramic and polymer with random distribution of carbon fibers in that region.

3.2. Anisotropic Thermal Conductivity of CNT/ceramic Thin Film

The anisotropic thermal conductivity of the CNT/ceramic thin film was characterized using TDTR method. Figure 6 shows the experiment raw data and the heat transfer model fitting results. A three-dimensional heat transfer model was used to calculate the temperature rise on the top surface and the measured signal. Other parameters in the model such as the heat capacity and the thicknesses of the aluminum (Al) film and the CNT/ceramic film were also determined. For example, the thickness of the Al film was determined by the acoustic echoes in the signal, shown in Figure 7. Since heat propagating in the sample will generate strain field, and thus acoustic waves, the travelling time of the acoustic waves can be determined, so as the thickness of the thin film. Then through numerical fitting, we then adjusted the unknown thermal conductivity to match the experimental signal data. Through this way, the thermal conductivity was be extracted. Since two measurements were carried out along different directions of the samples, the anisotropic thermal conductivity of this sample was obtained. The measurement results show that the thermal conductivity is 7.2 ± 0.7 W/mK in the in-plane direction, and 2.0 ± 0.2 W/mK in the through-thickness direction. The thermal anisotropy ratio is about 3.6, which is due to the preferable alignment of CNTs in the in-plane direction. This result is an indication that the CNT/ceramic film can help better dissipate heat in the in-plane direction on time before penetrating into the sample.

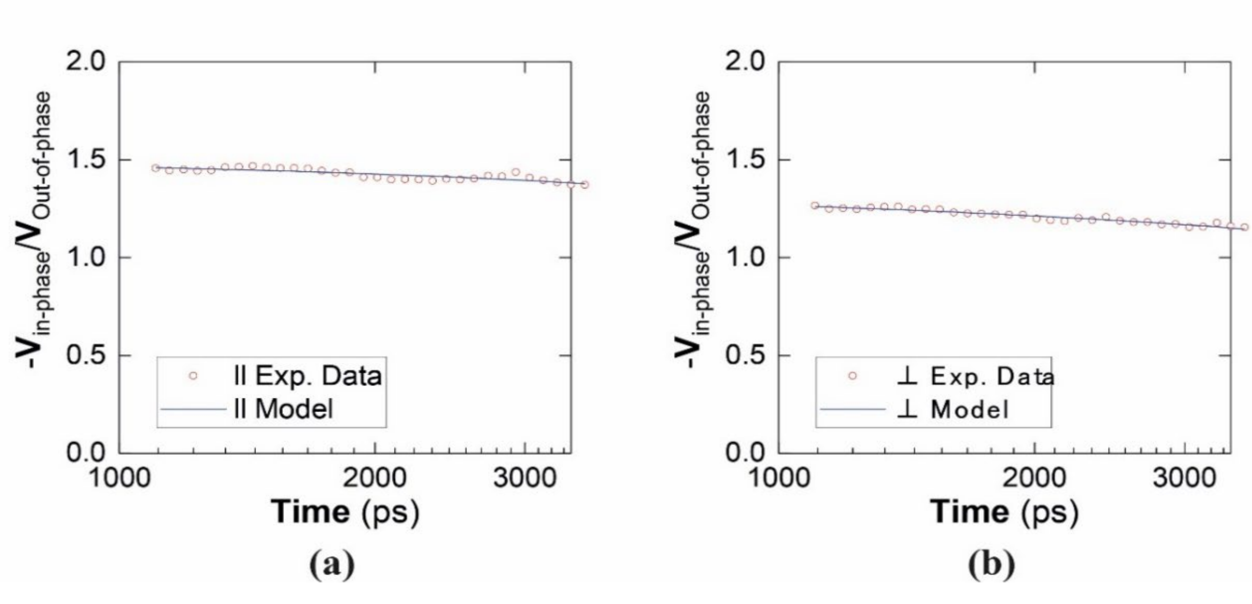

Figure 6: TDTR data with fitting model of the (a) parallel and (b) perpendicular samples

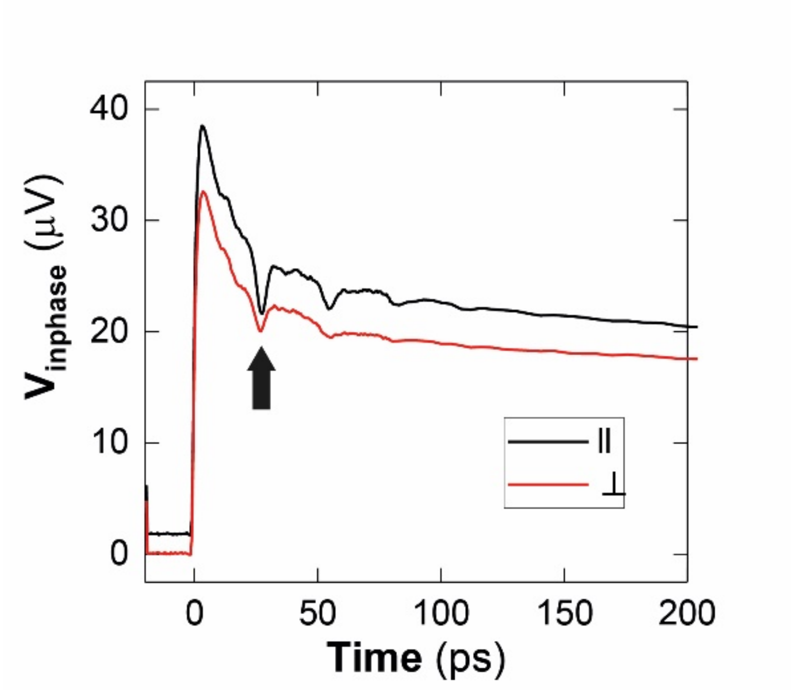

Figure 7: The in-phase signal of the TDTR data. The arrow is the downward acoustic echo at the interface between metallic film and the sample (27 ps).

Finite element analysis method was then used to analyze the temperature profile in the sample when the top surface experiences a sudden change of temperature. In the simulation, we assume the other areas of the surface are maintained at 60 °C due to the heat exchange with the environment and the top surface will change its temperature at time t=0. Three cases were considered: (a) the top surface has a constant 135 °C temperature when t>0; (b) a 100-micron-diameter heat source heats the top surface; (c) the top surface has a periodic heating with a squared-wave shape and the highest temperature at 135 °C. Figure 8 shows the simulation results. We monitored the temperature between the top layer and the back of the sample (opposite side) and found that this temperature is always less than 100 °C.

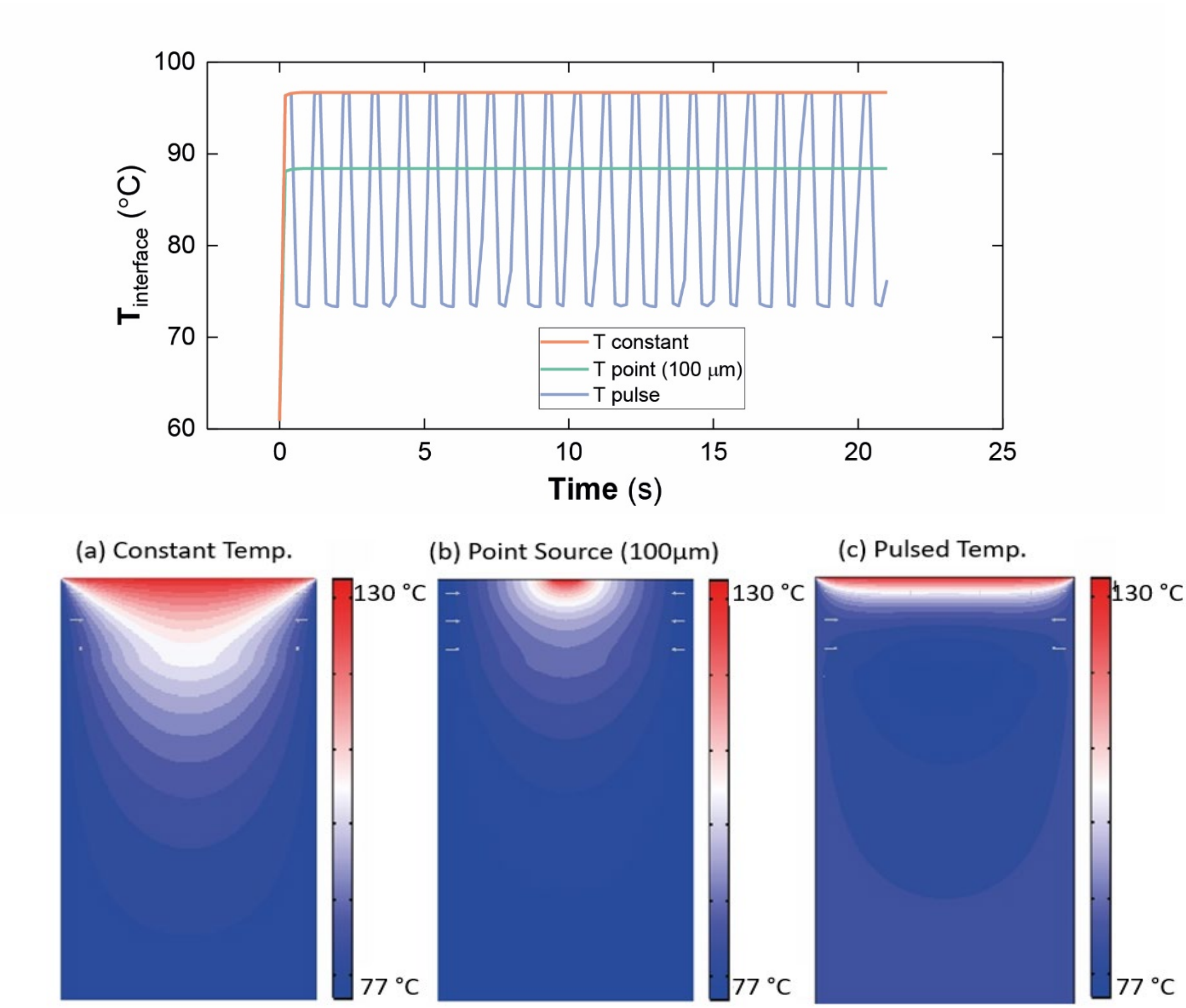

Figure 8: The transient temperature at the interface. The light red, the light green, and the light blue line is the result with (a) the constant temperature on the top surface, (b) the constant temperature on the point (100 ㎛), and (c) the pulsed constant temperature on the top surface.

3.3. Temperature Measurement at the Interface

Based on the experimental set-up described in section 2.3, temperature distribution in two different directions and points for the hybrid composite were determined. The sample's dimension for this experiment is described in Figure 9 (a). The heater's temperature was maintained at 125 ± 0.2 ºC and the measurement was recorded for 10 minutes. The distance from the heater was also set at 6 mm. From the results as shown in Figure 9 (b), the temperature in the in-plane direction at 6 mm from the heater is maintained at 93 ± 0.4 ºC and the temperature at the back of the sample in the through-thickness direction is maintained at 75 ± 0.5 ºC for 10 minutes.

Afterwards, we used the result from the experiment to simulate and predict the temperature at steady state at the interface using COMSOL multi-physics software. The conditions for the geometry were the same as the experiment and the material properties used for the simulation were based on the experimental values obtained and values from theoretical assumptions. For example, it was assumed that the sample has a smooth surface between each layer, so that the thermal conductance at the interface can be taken as 80 MW/m^{2}k. Also, since it is difficult to prepare an independent transition layer and measure its properties, we assumed that the through-thickness thermal conductivity of the transition layer is 1 W/mk which is the same for CFRP. All other parameters for the simulation are described in Table 1. Figure 10 presents the simulation result showing the temperature distribution in the system at the interface when the temperature of the heater is maintained at 125 ºC. From the curve, the temperature at the interface reached steady state at around 114 ºC. This result is an indication that the protective system can provide good thermal protection to CFRP by reducing the amount of heat travelling in the through-thickness direction. It is worth noting that this protective system is around 100 µm. The thermal protection performance is expected to be improved with increased thickness.

Table 1: Material properties used for the simulation

(E and T indicate experimental and theoretical values respectively)

Properties		
Thermal Conductance^T (G′)	CNT/ceramic-transition layer interface: 80 MW/m^{2}k	Transition layer-CFRP interface: 80 MW/m^{2}k
Temperature^E (T)	T_{bottom}= 75 ºC	T_{beam}= 125 ºC
Thermal conductivity (k) z-direction	CNT/ceramic film^E 2 W/mk	CFRP and transition layer^T 1 W/mk

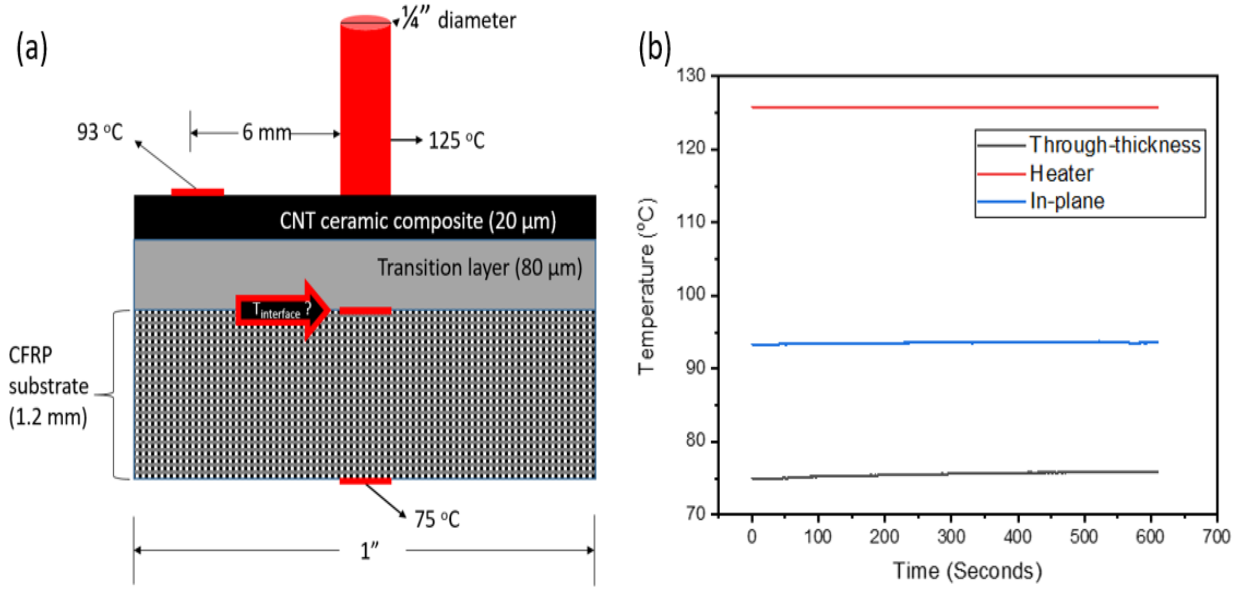

Figure 9: (a) Schematic representation of the geometry conditions for both experimental and simulated temperature profiling and (b) plot of raw experimental data from the test

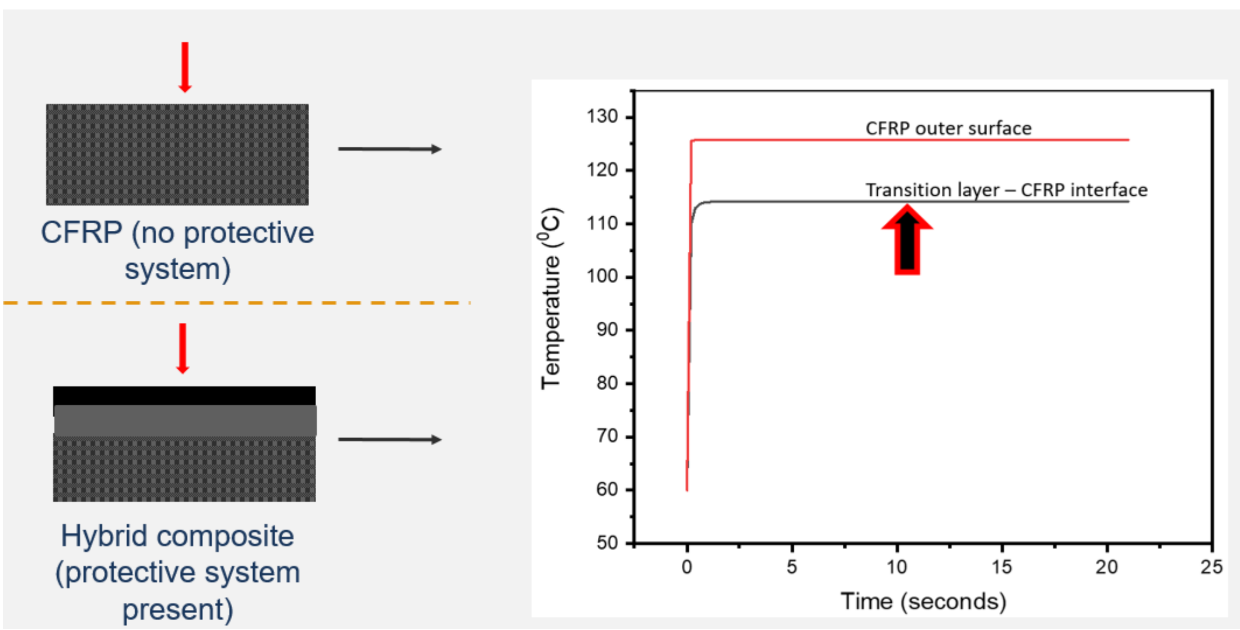

Figure 10: Comparison between temperature profiles at the interface of hybrid composite with the exterior surface of CFRP

4. CONCLUSION

In this project, we have developed a hybrid multifunctional composite material that is an improvement upon the thermal of traditional polymer composites. Such hybrid composite materials can be applied in higher temperature and harsher environment than current typical polymer-based composites and can be utilized especially in naval and marine parts for enhanced strength and durability. This hybrid composite is composed of a protective skin material of flexible CNT/ceramic film bonded through co-curing process onto the surface of CFRP to improve its survivability in adverse environments. The microstructural characterization show ceramic and polymeric matrices are evenly distributed and interlocked each other by the carbon fibers in the transition layer.

Thermal property investigations reveal that this protective layer can offer exceptional thermal protection to CFRP. For instance, the anisotropic thermal property result show that the thermal conductivity is 7.2 ± 0.7 W/mK in the in-plane direction, 2.0 ± 0.2 W/mK in the through-thickness direction, and anisotropic thermal ratio of 3.6. This result indicate that the CNT/ceramic layer can better dissipate heat in the in-plane direction rather that penetrating into the substrate. Another thermal investigation reveals that the temperature at the transition layer – CFRP interface can be minimized to around 114 ^{o}C when the exterior surface of CNT ceramic film is heated to 125 ^{o}C. These results indicate that the protective system can better help protect CFRP in harsh thermal environments.

References

[1] Adam Quilter. “Composite in Aerpspace Application”. Aviation Pros, October 2004. <https://www.aviationpros.com/article/10386441/composites-in-aerospace-applications>

[2] Pramanik A. Basak A.K., Dong Y., Sarker P.K., Uddin M.S., Littlefair G. Dixit A.R., Chattopadhyaya S. “Joining of carbon fiber reinforced polymer (CFRP) composites and aluminium alloys – A review”. *Composites Part A* 101 (2017): https://doi.org/10.1016/j.compositesa.2017.06.007

[3] Mallick P.K. *Fiber Reinforced Composites: Materials, Manufacturing, and Design, 3rd Ed*. CRC Press, 2007.

[4] Rallini Marco, Natali Maurizio, Monti Marco, Kenny M. Jose, Torre Luigi. “Effect of alumina nanoparticles on the thermal properties of carbon fiber-reinforced composites”. *Fire and Materials* 38 (3) (2014): 339-355. https://doi-org.prox.lib.ncsu.edu/10.1002/fam.2184

[5] Levchik Sergei V., Weil Edward D. “Thermal decomposition, combustion and flame-retardancy of epoxy resins—a review of the recent literature.” *Polymer International* 53 (2004): 1901–1929. https://doi-org.prox.lib.ncsu.edu/10.1002/pi.1473

[6] Maurer, C., Schulz, U. “Erosion resistant titanium based PVD coatings on CFRP”. *Wear* 302 (2013): 937–945. https://doi.org/10.1016/j.wear.2013.01.045

[7] Lee, C.K. “Structure, electrochemical and wear-corrosion properties of electroless nickel phosphorus deposition on CFRP composites”. *Material Chemistry & Physics* 114 (1) (2009): 125–133. https://doi.org/10.1016/j.matchemphys.2008.08.088

[8] Ganesan Amirthan, Okada Takumu, Motohiro Yamada, Masahiro Fukumoto. “Microstructure and mechanical properties of warm-sprayed titanium coating on carbon fiber-reinforced plastic”. *J. Thermal. Spray Technology* 25 (4) (2014): 236–244. DOI: 10.1007/s11666-016-0392-x

[9] Moridi, A., Hassani-Ganngaraj S.M., Guagliano, M., Dao M. “Cold spray coating: review of material systems and future perspectives”. *Surface Engineering* 30 (6) (2014): 369-395. https://doi.org/10.1179/1743294414Y.0000000270

[10] Cho Durk Hyun and Lee Dai Gil. “Manufacturing of co-cured composite aluminum shafts with compression during co-curing operation to reduce thermal stresses” Journal of Composite materials 38 (1998): 1221-1241. https://doi-org.prox.lib.ncsu.edu/10.1177/002199839803201205

[11 Shin Kum Cheol, Lee Jung Ju and Lee Dai Gil. “A study on the lap shear strength of a co-cured single lap joint”. *Journal of Adhesion Science and Technology* 14 (2000): 123-139. 10.1163/156856100742140

[12]Ju Licheng, Yang jinshan, Hao Ayou, Daniel Justin, Morales Justin, Nguyen Spencer, Andrei Petru, Liang Richard, Hellstrom and Xu Chengying. “A hybrid ceramic-polymer composite fabricated by co-curing lay-up process for a strong bonding and enhanced transient thermal protection”. *Ceramics International* 44 (10) (2018): 11497-11504. https://doi.org/10.1016/j.ceramint.2018.03.211

[13] Cahill D. G. "Analysis of heat flow in layeres structures for time-domain thermoreflectance". *Review of Science Instruments* 75 (12) (2004): 5119-5122. https://doi.org/10.1063/1.1819431

[14] Kang K., Koh Y. K., Chiritescu C., Zheng X. and Cahill D. G. "Two-tint pump-probe measurements using a femtosecond laser oscillator and sharp-edged optical filters". *Review of Science Instruments* 79 (11) (2008): 114901. DOI: 10.1063/1.3020759

[15] Schmidt A. J., Chen X. and Chen G. "Pulse accumulation, radial heat conduction, and anisotropic thermal conductivity in pump-probe transient thermoreflectance". *Review of Science Instruments* 79 (11) (2008): 114902. https://doi.org/10.1063/1.3006335

[16] Zhu J., Tang D., Wang W., Liu J., Holub K. W. and Yang R. "Ultrafast thermoreflectance techniques for measuring thermal conductivity and interface thermal conductance of thin films". *Journal of Applied Physics*. 108 (9) (2010): 094315. https://doi.org/10.1063/1.3504213

[17] Puquing Jiang, Xin Qian, and Ronggui Yang. "Tutorial: Time-domain thermoreflectance (TDTR) for thermal property characterization of bulk thin film materials". Journal of Applied Physics 124 (2018): 161103. https://doi.org/10.1063/1.5046944